



Materials Science

An Indian Journal

Full Paper

MSAIJ, 13(5), 2015 [163-174]

Effect of reversed cyclic stressing and phase transition on the transient and steady state creep behavior of Al – 22 wt% Ag alloy

M.A.Mahmoud

Physics Department, Ain - Shams University, P.O. Box 5101, Heliopolis 11771, Roxy, Cairo, (EGYPT)

E-Mail: moustafa_a_mahmoud@hotmail.com

ABSTRACT

Static and completely reversed cyclic creep acceleration characteristics of Al – 22 wt% Ag alloy were investigated using a modified tensile testing machine. Different amplitudes of reversed cyclic stress (σ_{rev}) ranging from 7.2 to 10.2 MPa at different working temperatures ranging from 353 K to 413 K were performed. To get a relation between aging temperature and threshold stress (σ_{th}) for cyclic creep acceleration, aging temperatures ranged from 423 to 683 K were used. The transient creep and steady state creep parameters (n , β and $\dot{\epsilon}_{st}$) were calculated. Values of n , β and $\dot{\epsilon}_{st}$ showed a dependence on aging temperature and were found to increase with increasing σ_{rev} as well as working temperature. Transmission electron microscopy (TEM) is used to investigate the microstructures formed in the aged samples. The results were explained in view of mode of interaction between the thermally induced structures during aging with moving dislocations induced by the static stress or dislocation structure induced by cyclic stress. The value of the steady state creep exponent depicts high dependence of the steady state creep stage on transient creep stage. Precipitate-dislocation interactions are suggested as the rate controlling mechanism for both transient and steady state creep stages.

© 2015 Trade Science Inc. - INDIA

KEYWORDS

Creep;
Cyclic stress;
Al-Ag alloys;
Dislocations;
Phase transformation.

INTRODUCTION

Al – Ag based alloys with high performance are widely used in many fields because of their high thermal and electrical conductivity, high strength and easy casting. In particular, these alloys are required in studies concerning structure-property correlation and are widely applied to make very good predictions for elastic and plastic properties as function of volume fraction, shape and distribution of second

phase^[1]. Al – Ag alloy solutionized in the single-phase α region and aged within the metastable solvus typically exhibits the following precipitation sequence^[2]: GP zones (η - state and ϵ - state) \rightarrow metastable γ' -phase \rightarrow equilibrium γ - phase. From precipitation sequence, the spherical coherent GP zones are the first metastable phase to form. According to the constitutional diagram, aging Al – Ag alloy below 443 K forming initially the ordered η - state of GP zones while aging above 448 K produces the

Full Paper

disordered ε -state of zones^[3]. On heating at the intermediate stage of aging (above 493 K) the coarsening of GP zones takes place simultaneously with the formation of γ' -phase^[4]. Based on thermal treatments, the existence of GP zones and γ' -precipitates formed at early stages of aging is surmised while in later stages γ -phase become directly detectable^[5]. The transformation from γ' -phase to γ -phase occurs above ~ 648 K through a gradual loss of coherency by the generation of misfit dislocation^[6]. γ' - and γ -phases have the same composition of hexagonal structure (Ag_2Al), but they are slightly differing in lattice parameters^[7].

Creep characteristics are closely related to the internal microstructure of the testing material and used to determine the deformation and relaxation mechanisms associated with the kinetics of precipitates exist in binary alloys. The alteration in the levels of creep parameters provides insight into the role which the aging temperature plays in the precipitate formation and coarsening kinetics. Cyclic creep tests (creep tests with continuous and gradual changes in the applied stress) fill a significant position in mechanical testing of materials. Studies have been done on static and partial cyclic creep reduction in pure Al^[8, 9], various aluminum alloys^[10-14], copper^[15], lead^[16] and nickel^[17]. When the creep curves indicate larger creep rates under cyclic stress as compared to static stress of the same peak value, the behavior is termed cyclic creep acceleration. Cyclic stress retardation is referred to the state in which creep rates are very much smaller under cyclic stress

as compared to static stress of the same peak value.

Mechanical tests were carried out^[18] to show the effect of low frequency of partial cyclic stress reduction on the creep behavior of Al – Ag regime. Several important issues remain to be answered regarding the effect of completely reversed cyclic stress amplitudes (σ_{rev}) on the mechanical properties of Al – Ag alloy during phase transformations. Therefore, the object of the present work is to clarify the effect of crystal structure, morphology of the second phases and amplitudes of σ_{rev} on the creep behavior of Al – 22 wt% Ag.

EXPERIMENTAL

Al – 22 wt% Ag alloy was prepared in an induction furnace under vacuum using pure aluminum and silver (99.99%) as starting materials. Results from chemical analysis indicated that the final alloy composition is very close to the nominal one. The cylindrical ingots obtained were initially annealed for $\sim 4.32 \times 10^5$ sec at 850 K for homogenization and cooled at about 1.6×10^{-3} K sec⁻¹. The ingots were then machined into wires of 3.5×10^{-4} m in diameter for creep measurements and strips of 2×10^{-4} m thick for transmission electron microscopy (TEM) investigations. To get fairly similar samples free from pre-deformation due to the successive processes of swaging, the samples were underwent an additional anneal for 1.8×10^4 sec at 800 K and quenched in iced water. Immediately, the quenched samples were aged for 3.6×10^3 sec at different temperatures $T_a =$

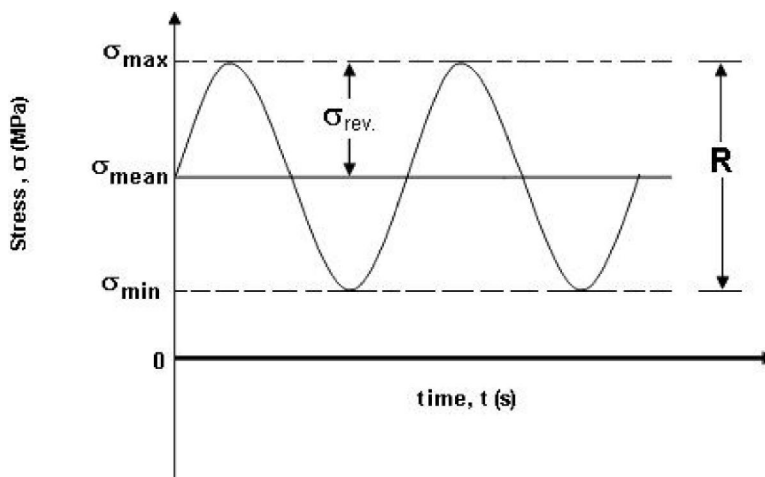


Figure 1 : Stress-time variation for completely reversed cyclic stress

423, 453, 493, 563, 613 and 683 K to generate the desirable microstructures required of GP zones, metastable γ' - and equilibrium – precipitates.

Creep runs were performed using a domestic made machine modified so that creep tests under either static stress or reversed cyclic stress can be done. The modifications added to the static creep machine are demonstrated elsewhere^[19]. The creep experiments were carried out under both static mean stress, $\sigma_{\text{mean}} = 56$ MPa and reversed cyclic stress of different amplitudes, $\sigma_{\text{rev}} = 7.2, 8, 10, \text{ and } 11.2$ MPa superimposed upon the static stress at working temperatures, $T_w = 353, 373, 393$ and 413 K. The reversed cyclic stress has the form of a sinusoidal wave of unique frequency = 0.44 Hz as shown in Figure 1 where the stress variation (R) used = $2 \sigma_{\text{rev}} = \sigma_{\text{max}} - \sigma_{\text{min}}$, and the mean stress (σ_{mean}) used = $(\sigma_{\text{max}} + \sigma_{\text{min}})$. σ_{max} and σ_{min} are the maximum and minimum stresses affecting the sample during cyclic creep respectively. To maintain equilibrium state, the sample was brought to the required working temperature at least for 300 sec prior to application of load. After applying the load, the creep data are not reported for the first 30 sec of each test to avoid the rise time of the load history. The initial 300 sec of each test were continuously captured carefully since that time nearly equals the time taken by transient creep stage. Strain was measured using a full bridge of two discrete strain gauges of length 25×10^{-3} m. The accuracy of temperature and elongation measurements is of the order ± 1 K and 1×10^{-6} m respectively.

Strips for TEM observations were thermally heated according to the experimental conditions. For ultimate thinning down to perforation, electro-polishing using a twin jet machine (Lectropol-5, struers) was done in a 10% perchloric acid and 90% ethanol solution at 273 K. The voltage and current values were around 13 – 19 V and 8 – 14 mA respectively. The perforated thin foils were subsequently rinsed in pure acetone then in distilled water and dried. The TEM investigations were performed on a JOEL – 100S transmission electron microscope.

RESULTS

In view of preliminary experiments, the author

found that there is a minimum value of σ_{rev} – hereafter denoted as threshold stress (σ_{th}) – must be superimposed upon the mean stress to initiate the cyclic creep acceleration. When the value of σ_{rev} was lower than σ_{th} value, the creep rate went to a rate equal to that in static creep. Therefore, in the present study the values of σ_{rev} were chosen to have values larger than σ_{th} values. The method used to obtain σ_{th} values was previously discussed by the same author^[14]. The values of σ_{th} in the present study were found to range between 3.32 and 4.33 MPa depending on the aging temperature only. The isothermal strain-time relations for samples of Al – 22 wt% Ag alloy aged for 3.6×10^3 sec at temperatures ranged from $T_a = 423$ K to 683 K were obtained under various amplitudes of σ_{rev} ranged from 7.2 MPa to 11.2 MPa and working temperatures ranging from 353 K to 413 K. The strain, ϵ of all creep tests was recorded with time until fracture occurs by necking. Representative creep curves for samples pre-aged at 423 K and 683 K under different amplitudes of σ_{rev} at constant working temperature = 413 K are shown in Figure 2a. The static creep curves (with $\sigma_{\text{rev}} = 0$) are also drawn on the same scale for comparison. Since the present study is concerned only with transient creep and steady state creep stages, so drawing of creep time is terminated at 120 min. Data obtained from Figure 2a showing the strain-time relations for transient creep stage are shown in Figure 2b. From Figure 2, it is worth noting that: i) the transient stage is characterized by a short duration time ($\sim 3 - 5$ min). ii) The creep strain – in both transient and steady stages – has been increased by increasing the amplitude of σ_{rev} . iii) Higher amplitudes of σ_{rev} yield shorter creep time.

Straight lines relate the logarithm of the experimental transient strain ($\ln \epsilon_{\text{tr}}$) against the logarithm of the transient creep time ($\ln t$) for different amplitudes of σ_{rev} at different aging and working temperatures were obtained from Figure 2b. The obtained linear relations have strong positive correlation coefficients and indicate that the transient creep could be represented by the equation^[20]:

$$\epsilon_{\text{tr}} = \beta (t_{\text{tr}})^n \quad (1)$$

Where t_{tr} is the transient creep time in seconds, n

Full Paper

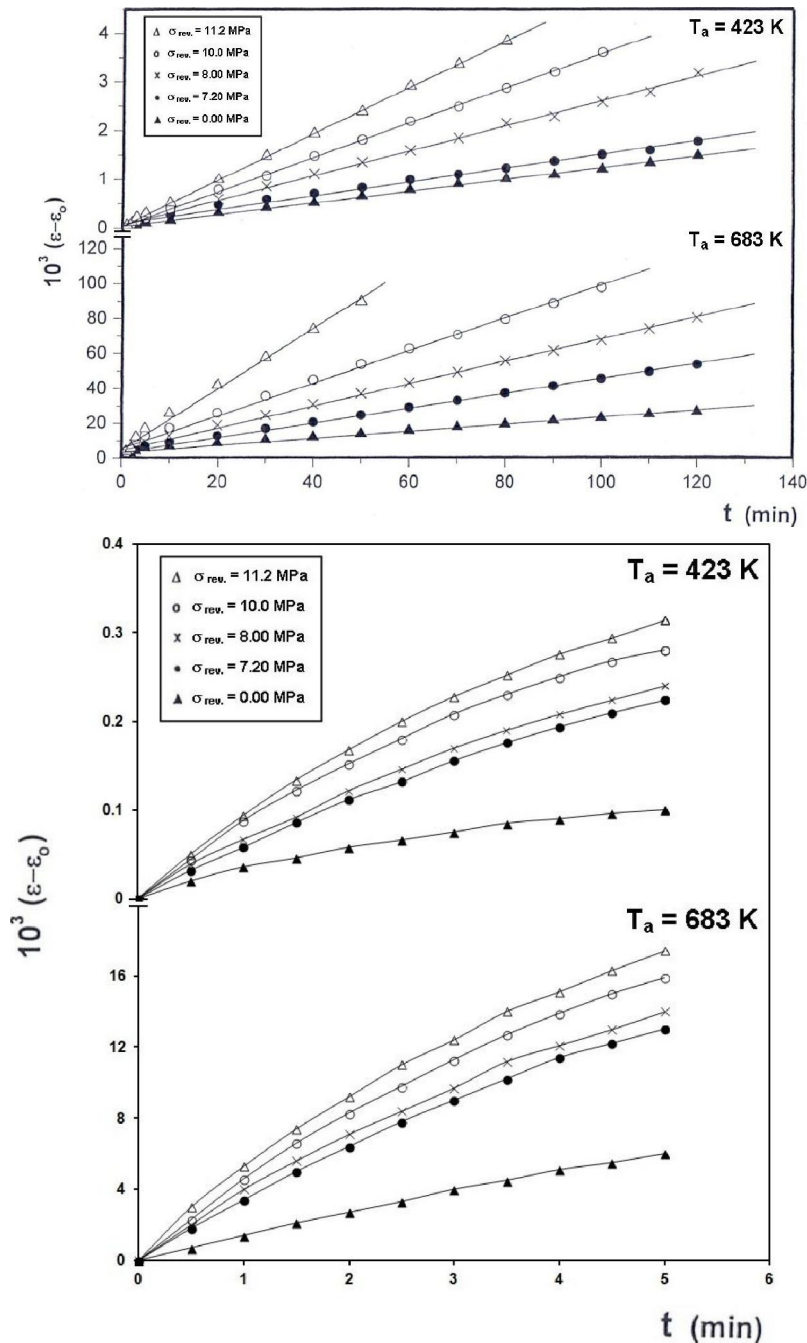


Figure 2 : (a) Representative creep curves obtained at working temperature of 413 K for Al-22 wt% Ag alloy samples crept under different amplitudes of σ_{rev} . ϵ_0 is the strain corresponding to the creep time = 0. (b) The data from Figure 2a showing differences in transient stage creep behavior at the same testing conditions

and β ? are the transient creep parameters. Slopes of the straight lines relating $(\ln \epsilon_{tr})$ and $(\ln t)$ yield the parameter n while the intercepts of the extrapolated lines towards $\ln \epsilon_{tr}$ axis yield the time independent creep parameter β . The constants n and β were governed by the test conditions. The dependence of n and β on aging temperature (T_a) for different amplitudes of σ_{rev} at different working temperatures (T_w)

is given in Figs. 3 and 4 respectively. The slopes of the linear parts of the plain creep curves of Figure 2a gives the steady state strain rate ($\dot{\epsilon}_{st}$) of the crept samples. The dependence of steady state strain rate, $\dot{\epsilon}_{st}$ on aging temperature (T_a) for different amplitudes of σ_{rev} at different working temperatures is shown in Figure 5.

The following obvious signatures can be noticed

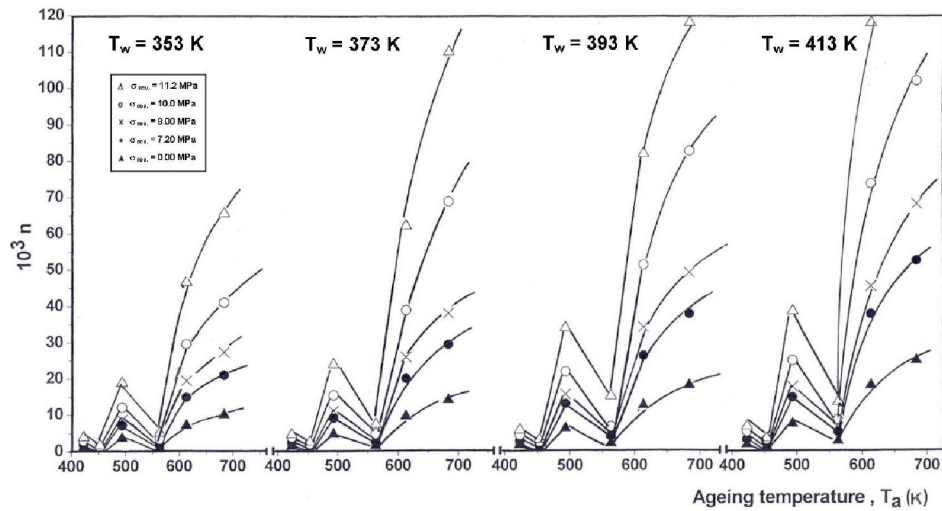


Figure 3 : The aging temperature dependence of the transient creep parameter n at different values of σ_{rev} . Working temperatures, T_w are indicated

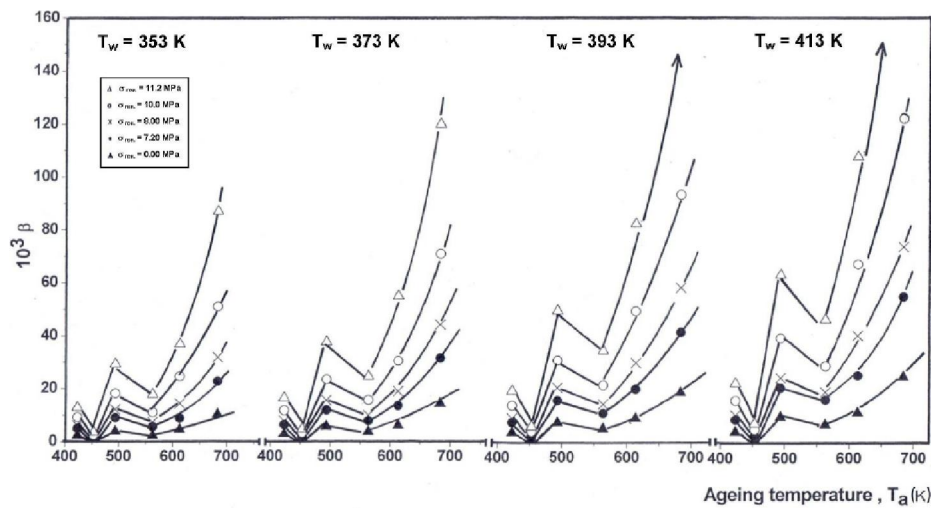


Figure 4 : The aging temperature dependence of the transient creep parameter β at different values of σ_{rev} . Working temperatures, T_w are indicated

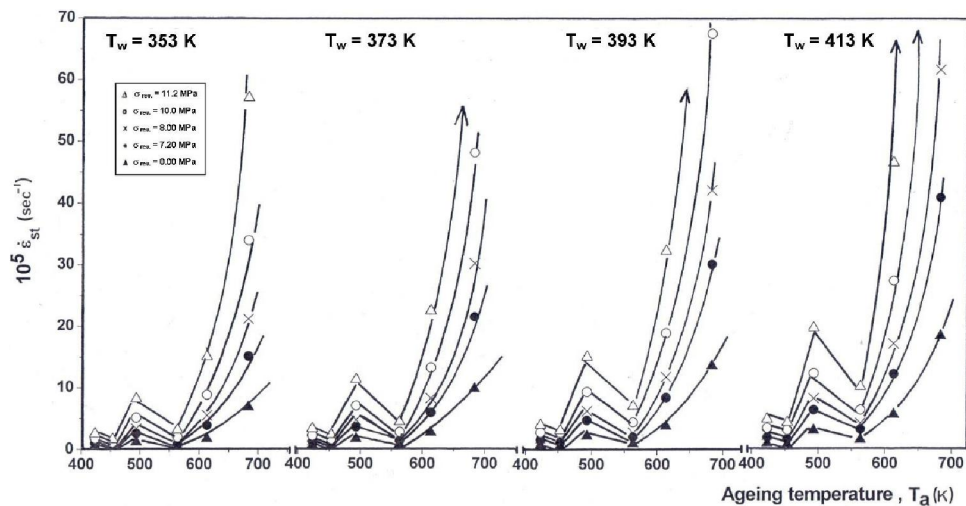


Figure 5 : The aging temperature dependence of the creep parameter $\dot{\epsilon}_{st}$ at different values of σ_{rev} . Working temperatures, T_w are indicated

Full Paper

from Figures 3 – 5:

- Higher values of n , β and $\dot{\epsilon}_{st}$ were observed with increasing aging temperature except at $T_a = 453$ K and 563 K.
- An increasing of n , β and $\dot{\epsilon}_{st}$ occurs in three aging temperatures ranges; (453 K – 493 K), (563 K – 613 K) and (613 K – 683 K), while the decrease in the same parameters occurs in the two aging temperature ranges; (423 K – 453 K) and (493 K – 563 K).
- For samples aged at 613 K and 683 K, a monotonic increase in n , β and $\dot{\epsilon}_{st}$ parameters was observed.
- For samples aged at $T_a = 453$ K, values of n , β and $\dot{\epsilon}_{st}$ exhibited smaller values than those aged at $T_a = 563$ K.
- The levels of n , β and $\dot{\epsilon}_{st}$ for samples aged at $T_a = 493$ K exhibited higher values compared with the levels for samples aged at 423 K.
- Under the same testing conditions, the higher working temperatures yielded higher values of n , β and $\dot{\epsilon}_{st}$.

Figure 6 depicts the influence of σ_{rev} on the creep parameters (n , β and $\dot{\epsilon}_{st}$) at different aging temperatures where increasing of σ_{rev} amplitudes is associated with quite similar increase in n , β and $\dot{\epsilon}_{st}$ values. However; such increasing is more pronounced at higher amplitudes of σ_{rev} .

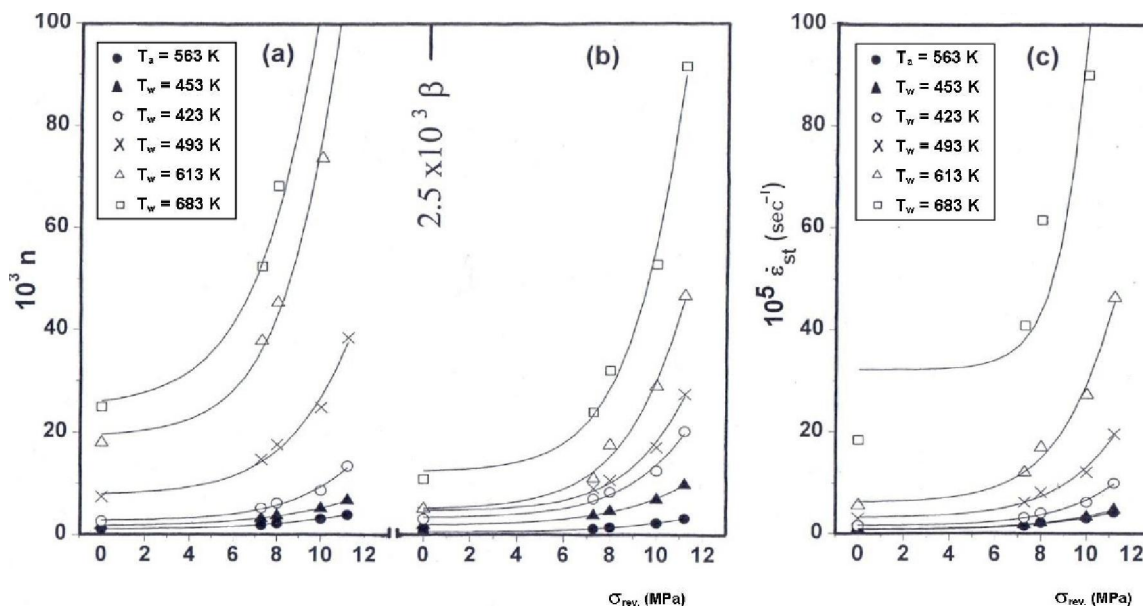


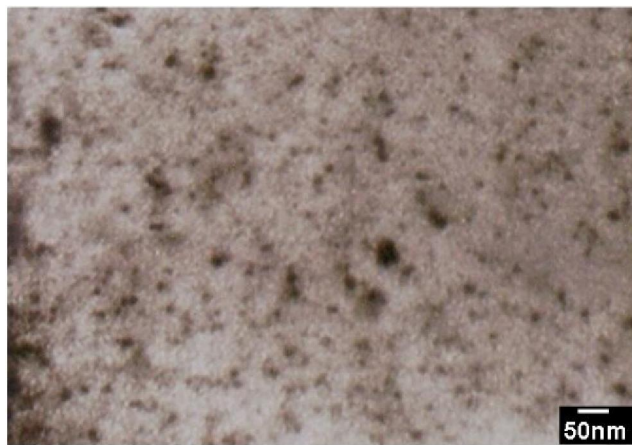
Figure 6 : (a, b and c): The σ_{rev} dependence of the creep parameters n , β and $\dot{\epsilon}_{st}$ respectively at different aging temperatures, T_a

Figures 7 – 9 illustrate the development of the microstructure during aging samples at different temperatures for 3.6×10^3 sec. Figures. 7a and 7b show the precipitates of GP zones in samples aged at 423 and 493 K respectively. Figure 8a shows coarsened GP zones close to γ' - precipitates in samples aged at 563 K, while Figure 8b shows coarsened γ' - plate-like precipitates taken for samples aged at 613 K. Figure 9 shows γ - precipitates taken for samples aged at 683 K.

DISCUSSION

Thermal and strain hardening are the main techniques used to improve the strength of Al – Ag alloy without losing its ductility. In the present creep results, the interaction of moving dislocations with GP zones, γ' - and γ - phases controls the strengthening process and work hardening mechanism. The aging temperature dependence of the values of n , β and $\dot{\epsilon}_{st}$ (Figures. 3 – 5) depicts non linear relations and can be divided into five aging temperature ranges:

In the first aging temperature range ($T_a = 423$ K to 453 K), the decomposition of quenched supersaturated solid solution starts precipitation with intense fine ordered η - state GP zones up to 423 K and the disordered ϵ - state zones above this temperature to 453 K^[21-23]. Such tiny precipitates of



(a)



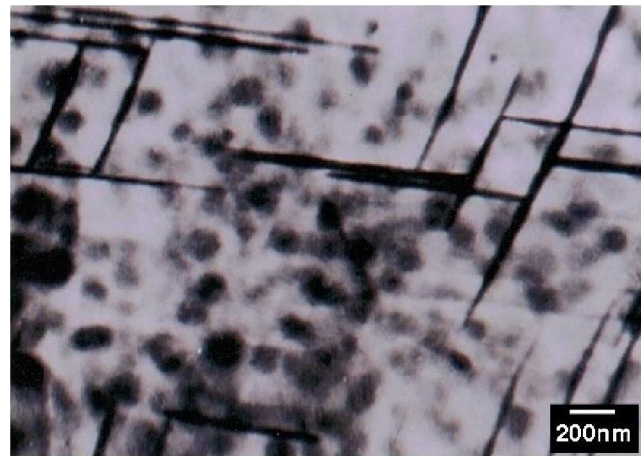
(b)

Figure 7 : TEM micrographs showing the precipitation of GP zones in samples aged respectively at a) 423 K and b) 493 K

zones (see Figure 7a) act as impeding agents for moving dislocations and causing retardation of their motion resulting in a high creep resistance behavior i.e. lower values of n , β and $\dot{\epsilon}_{st}$ [24-26].

In the second aging temperature range ($T_a = 453$ K to 493 K), the formation of fine GP zones is drastically reduced and growth of zones become the dominate kinetics [27, 28]. The partial dissolution and subsequent coalescence of GP zones are achieved on the expense of their number (see Figure 7b). The coarse GP zones of small numbers and small density provide small barriers to dislocation motion resulting in a relatively lower strength i.e. increasing of n , β and $\dot{\epsilon}_{st}$ values [29].

In the third aging temperature range ($T_a = 493$ K to 563 K), the elimination of most of GP zones and existence of nucleation sites for a huge number of



(a)



(b)

Figure 8 : TEM micrographs showing a) coarse GP zones close to γ^- precipitates in samples aged at 563 K and b) coarse γ^- plate-like precipitates for samples aged at 613 K

small sized γ^- precipitates is the most probable event [30]. Accordingly, a matrix with an oriented microstructure comprised regions with semi coherent γ^- precipitates (see Figure 8a) is easily produced [31]. The increased area of γ^- precipitates-matrix interfaces effectively inhibits the moving dislocations and improves strengthening process [31, 32].

In the fourth aging temperature range ($T_a = 563$ K to 613 K), the alloy goes immediately from formation of γ^- phase at the lower temperature (563 K) to growth and coarsening of γ^- plates above this temperature up to 613 K [33]. Such coarsening is associated with an increase in the precipitates thickness together with a decrease in their number (see Figure 8b). The diffusivity of coarsening semi-coherent γ^- precipitates within the matrix is expected

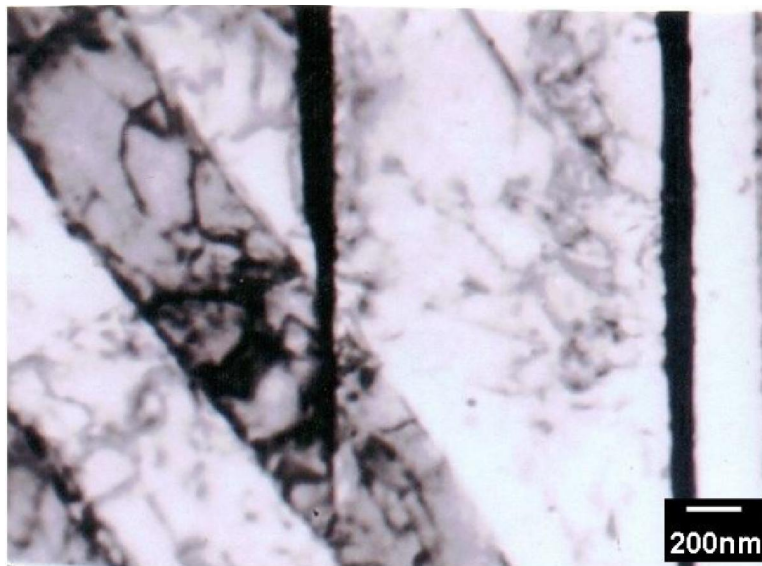


Figure 9 : TEM micrographs showing γ - precipitates for samples aged at 683 K

to increase the rate of recovery of dislocations at the interface boundary accompanied with a reduced flow stress state^[34].

Finally, in the fifth aging temperature range ($T_a = 613\text{ K to }683\text{ K}$), coarsening of γ -precipitates has ceased and formation of γ -precipitates becomes the dominant reaction yielding a continuous supply of solute Ag atoms^[35]. The Ag atoms drive out to matrix would prefer to attach the face of the formed γ -precipitates and thereby shift them towards their equilibrium shape^[36]. The large widely spaced composition of γ -precipitates (see Figure 9) will be less effective in holding up moved dislocations or inhibiting their slip leading to a monotonic increase in n , β and $\dot{\epsilon}_{st}$ values^[2]. This behavior is well agreement with previous results of the equilibrium θ -phase in Al-Cu alloys^[37].

From Figures 3 – 5, it is clear that under the same conditions of σ_{rev} and working temperatures, levels of the creep parameters (n , β and $\dot{\epsilon}_{st}$) for samples aged at 423 K are generally lower than those aged at 493 K. These results may be due to vacancy clusters formed at 493 K which enhance the coarsening of GP zones and reduce the precipitates-dislocation interactions. This structure enhances the creep parameters compared with small sized ordered η -state of GP zones formed at 423 K. The maximum strength achieved at $T_a = 453\text{ K}$ is reduced at $T_a = 563\text{ K}$, due to the formation of γ -precipitates of less number and small size. Formation of such struc-

ture makes the dislocation slip planes relatively clean of obstacles and allow larger slip distances for moving dislocations compared with disordered ϵ -state zones formed at 453 K. These results are in good agreement with the common reported data^[18,30].

The method used to calculate the values of σ_{th} for Al – Ag alloy was discussed in detail by the same author elsewhere^[14]. Using the same method in the present study, the values of σ_{th} were calculated and were found to range from 3.32 to 4.33 MPa depending only on aging temperature (T_a). When the calculated σ_{th} are normalized against the shear modulus for the crept samples (G) and related to the parameter of homologous temperature (T_a/T_m), a relationship is established for predicting the values of σ_{th} for cyclic creep acceleration. This relation has the form:

$$[T_a / T_m] [\sigma_{th} / G] = 1.116 \times 10^{-3} \quad (2)$$

The parameter of homologous temperature (~ 0.44 to 0.72 for the present study) is introduced to compensate the stronger dependence of σ_{th} on temperature more than the shear modulus G . The calculations indicate that equation (2) seems to describe the obtained results quite well within the experimental scatter for σ_{th} and G . So, provided that dislocation structure is reasonably constant within the aging temperature range of interest, the value of σ_{th} for cyclic creep acceleration would be predictable for different aging temperatures. Last equation ex-

plains now why it was decided to study the effect of σ_{rev} at different aging temperatures.

The cyclic creep behavior in polycrystalline Al and single crystal Al was found to be qualitatively similar, therefore the cyclic softening and hardening processes are not grain boundary related phenomena^[10]. The increased creep strain (cyclic creep acceleration) associated with the superimposed σ_{rev} as shown in Figures (2 – 6) might be due to the formation of new dislocation structure^[39]. At the beginning of transient stage i.e. during initial cycles, a dislocation structure of poorly developed cells more or less equiaxed with mid area free of dislocations is formed. The continuous cyclic stress forced the formed structure to develop cells have nearly wall-like shape comprised of relatively short and incomplete cell wall segments and lie along the traces of the most active slip system. As the transient creep time proceeds, cell wall structure composed of a mixture of tangles trapped dislocations and piled-up dislocations of the steady state slip systems is constructed^[38, 39]. Whilst such process, the fluctuations in the internal stresses during the unloading part of cycles enhance the cross-slip of transient mobile screw dislocation.^[12] Since the long range back stress upon reloading is insufficient to prevent the dislocations movement at positions away from the blocked regions in their slip plane, the cross

slipped screw segments are likely to move forward to provide new sources for strain during succeeding load cycles^[40]. As a result, an increase in the transient creep parameters (n and β) by a relatively higher rate is observed with the reversed cyclic stress applied i.e. a significant increase in sample ductility. Around the end of transient stage, the cell walls oriented along the traces of the steady state slip system become more dense and irregular in shape^[41]. Whenever the size of the cellular network structure becomes more homogeneous, the balance between the cross-slip of screw segments of dislocations and rearrangement of the obstacles to dislocation motion stimulates the initials of steady state creep stage. Increasing the amplitude of σ_{rev} would develop intensified cell walls structure oriented along the traces of the various slip systems associated with high strain sources^[10]. Such local intensifications and refinements of cell structures have been linked the observed rapid softening phenomenon. The shortness of the steady state stage by increasing of σ_{rev} might be due to the repeated micro slip on steady state system and subsequent rearrangement of the dislocations in the preferred orientation along cell walls^[41, 42].

The effect of working temperatures as observed in Figures 3 – 5 is in accordance with thermodynamics grounds and consistent with the nature of

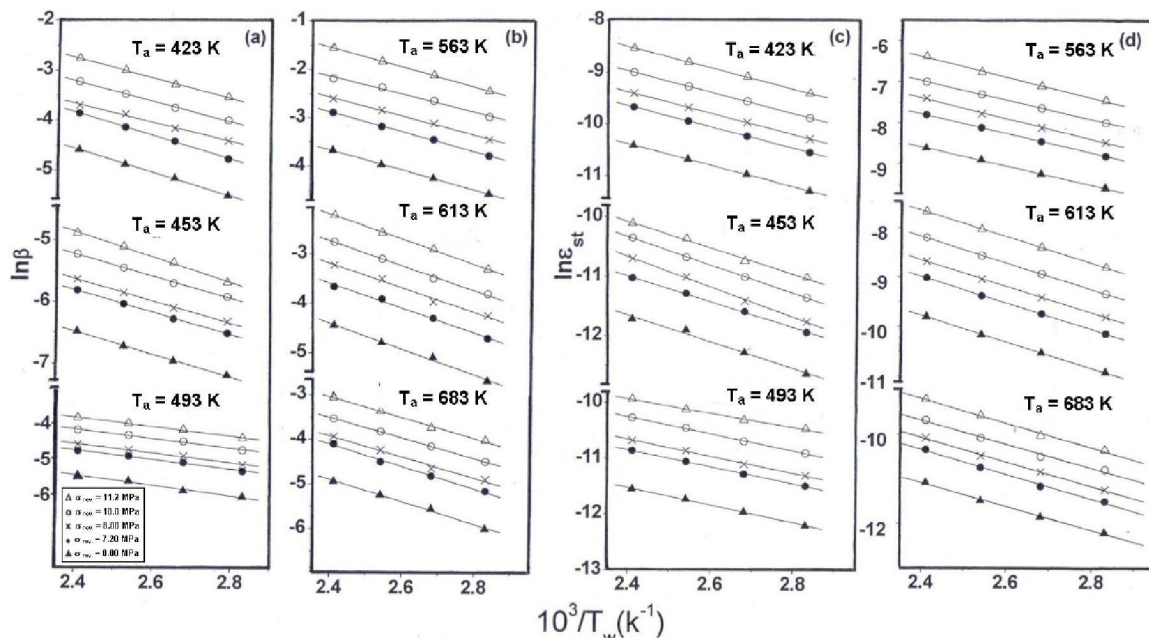


Figure 10 : The relation between both $\ln \beta$ (a, b) and $\ln \dot{\epsilon}_{st}$ (c, d) and $10^3/T_w$ at different amplitudes of σ_{rev}

Full Paper

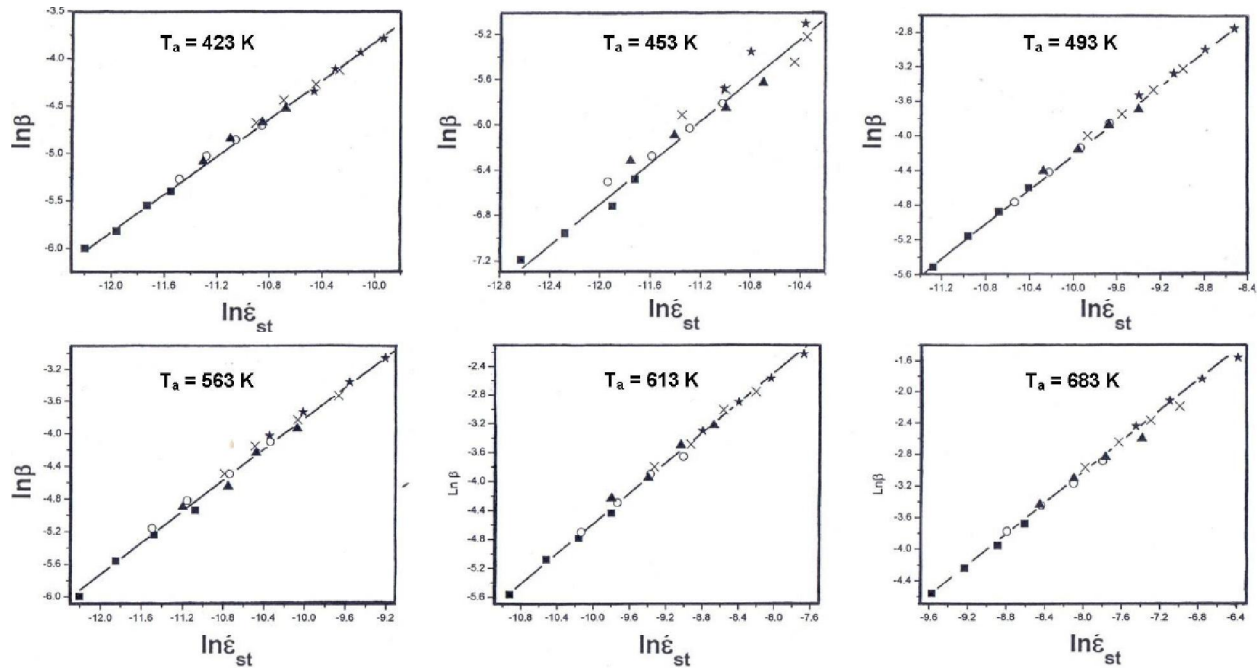


Figure 11 : The relation between $\ln \beta$ and $\ln \dot{\epsilon}_{st}$ at different aging temperatures, T_a . The values of σ_{rev} applied are *11.2 MPa, x 10 MPa, ▲ 8 MPa, O 7.2 MPa and ■ 0 MPa

creep process being a thermally activated process. The progress reduction of the strength with increasing working temperatures might be due to: i) the dislocation annihilation associated with the relaxation of dislocations at the front of the pile-ups at grain boundaries^[24]. ii) The regular succession of viscous motion of dislocations on their slip planes due to the decreasing of the interaction between the existing phases with moving dislocations^[38]. iii) The redistribution of dislocations in the network at transformation and formation of Frank-Read sources due to the release of stored deformation energy^[21].

$$\beta = \text{constant} \exp. \left(\frac{-E_{tr}}{RT_w} \right) \quad (3)$$

The activation energy of creep process can be calculated through the superposition of the creep parameters β and $\dot{\epsilon}_{st}$ with the working temperature (T_w) at which samples already worked on^[30]. This superposition –to form master curves– can be done through the application of the Arrhenius reported equations^[21]:

$$\dot{\epsilon}'_{st} = \text{constant} \exp. \left(\frac{-E_{st}}{RT_w} \right) \quad (4)$$

Where; R is the universal gas constant, E_{tr} and E_{st} are the energies (in kJ/mol) activating the transient

creep and steady state creep processes respectively. Plots of $(\ln \beta)$ and $(\ln \dot{\epsilon}_{st})$ versus $10^3 / T_w$ (K^{-1}) are constructed in Figure 10. Slopes of the well straight parallel lines resulted yield activation energies of small values ranged from 15 to 26 kJ/mol for transient creep stage (Figure 10 a&b) and from 17 to 29 kJ/mol for steady state creep stage (Figure 10 c&d). The values of activation energies are slightly affected by either the amplitudes of σ_{rev} or aging temperatures and predict the same responsible mechanism for both transient and steady state creep stages. The mechanism operates during the creep process is not a diffusion mechanism since a relatively large activation energy is required^[27]. It is more likely to the precipitate-dislocation interactions^[21-23, 33].

$$\beta = \beta_0 (\dot{\epsilon}'_{st})^\lambda \quad (5)$$

The dependence of the transient creep parameter β on the steady state creep strain rate $\dot{\epsilon}'_{st}$ was reported by many authors^[33, 43]. The relation concerning this dependence is:

where β_0 is a constant. λ is the steady state creep exponent and measured through the ratio $\lambda = (\partial \ln \beta / \partial \ln \dot{\epsilon}'_{st})$. Thus the slopes of the straight lines relating $(\ln \beta)$ and $(\ln \dot{\epsilon}'_{st})$ shown in Figure 11 give the values of λ which were found to range from 0.88 to 0.94 depending on aging temperatures. The comparatively

high values of λ (which tends to unity) affirm that both transient and steady state creep stages are extensively correlated even through the transformation regions, a matter that has been already confirmed through the measured values of activation energy for both stages.

CONCLUSION

1. Marked effect of imposed reversed cyclic stress amplitude (σ_{rev}) during creep of samples of Al – 22 wt% Ag alloy aged at different aging and working temperatures was observed.
2. The creep parameters n , β and $\dot{\epsilon}_{st}$ showed a dependence on either both aging and working temperatures or completely reversed cyclic stress amplitudes.
3. The strength variations during aging process of Al – Ag system above room temperature are mainly due to formation, growth and transformation of the phases existing at each temperature range.
4. The non linear changes in the creep parameters with aging temperatures have been interpreted using the dislocation creep models.
5. An expression predicts the value of σ_{th} for cyclic creep acceleration at different aging temperatures for the alloy under study is offered.
6. The observed cyclic creep acceleration is interpreted by a cyclic softening process involving dislocations on secondary systems.
7. The responsible mechanism for both transient and steady state creep stages is the precipitate-dislocation interactions.

REFERENCES

- [1] W.J.Poole, N.Charros; Mater.Sci.Eng.A, **406**, 300 (2005).
- [2] M.A.Mahmoud; Phys.Stat.Sol.(a), **186**, 143 (2001).
- [3] G.Dlubeck, G.wendrock, K.Pawelzyk; Phys.Stat.Sol.(a), **140**, 311 (1993).
- [4] A.Malik, B.Schonfeld, G.Kostorz, Z.Metallk; **88**, 625 (1997).
- [5] K.T.Moore, J.M.Howe, H.I.Aaronson, D.R.Veblen; Acta Mater., **50**, 943 (2002).
- [6] K.T.Moore, J.M.Howe, D.R.Veblen;

- Metall.Trans.A, **33**,1561 (2002).
- [7] R.M.Aikin Jr, M.R.Plichta; Acta metal.mater., **38**, 77 (1990).
- [8] F.Lorenzo, C.Laird; Acta Metall., **32**, 681 (1984).
- [9] D.Shetty, M.Meshii; Metall.Trans.A, **6**, 349 (1975).
- [10] T.Jaglinski, R.Lakes; Trans.ASME, **126**, 378 (2004).
- [11] W.Blum, A.Rosen, A.Cegielska, J.I.Martin; Acta Metall., **37**, 2439 (1989).
- [12] G.Graiss, M.A.Mahmoud, A.H.Ashry, A.M.Abdelkhalekh, A.F.Abd El-Rehim; Phys.Stat.Sol.(a), **201**, 2295 (2004).
- [13] F.Abd El-salam, A.M.Abdelkhalekh, R.H.Nada; Physica B, **388**, 219 (2007).
- [14] A.F.Abd El-Rehim, M.A.Mahmoud; Mater.Sci.Technol., **27**, 44 (2011).
- [15] A.H.Meleka, A.V.Evershed; J.Inst.Metals, **88**, 411 (1949).
- [16] J.N.Greenwood; Proc.ASTM, **49**, 834 (1949).
- [17] G.A.Webster, B.J.Picaiceyi; Trans.Am.Soc.Metals, **59**, 847 (1966).
- [18] M.A.Mahmoud, A.F.Abd El-Rehim; J.Mater.Sci., **45**, 1579 (2010).
- [19] A.F.Abd El-Rehim; Ph.D.Thesis, Ain Shams Univ.Cairo, Egypt, 68, (2004).
- [20] A.F.Abd El-Rehim; J.Mater.Sci., **43**, 1444 (2008).
- [21] M.A.Mahmoud; Physica B, **304**, 456 (2001).
- [22] G.H.Deaf, S.B.Yossef, M.A.Mahmoud; Phys.Stat.Sol.(a), **158**, 79 (1996).
- [23] G.H.Deaf, S.B.Yossef, M.A.Mahmoud; Phys.Stat.Sol.(a), **168**, 389 (1995).
- [24] T.Kanadani, A.Umada; Phys.Stat.Sol.(a), **148**, K23 (1995).
- [25] T.Kanadani, A.Umada; Phys.Stat.Sol.(a), **151**, K29 (1995).
- [26] R.H.Nada; Mater.Sci.Eng.A, **528**, 1233 (2011).
- [27] G.Graiss, M.A.Mahmoud; Fizika A, **9**, 137 (2000).
- [28] G.Graiss, M.A.Mahmoud; J.Mater.Sci., **36**, 1507 (2001).
- [29] G.H.Deaf, S.B.Yossef, M.A.Mahmoud, G.Graiss, M.A.Kenawy; Phys.Stat.Sol.(a), **158**, 471 (1996).
- [30] M.A.Mahmoud, G.Graiss; J.Mater.Sci., **37**, 2215 (2002).
- [31] K.K.Sagoe-Crentsil, L.C.Brown; Phil.Mag.A, **61**, 451 (1990).
- [32] F.Abd El-salam, M.A.Mahmoud, A.M.Abdelkhalekh, R.H.Nada; Physica B, **324**, 110 (2002).
- [33] G.Graiss, M.A.Mahmoud; Cryst.Res.Technol., **35**, 95 (2000).

Full Paper

- [34] K.K.Sagoe-Crentsil, L.C.Brown; *Phil.Mag.A*, **63**, 477 (1991).
- [35] K.T.Moore, J.M.Howe; *Acta Mater.*, **48**, 4083 (2000).
- [36] N.Nabarro, J.M.Howe; *Phil.Mag.A*, **63**, 645 (1991).
- [37] M.A.Mahmoud, A.H.Ashry, A.M.Abdelkhalekh, A.F.Abd El-Rehim, G.Graiss; *Cryst.Res.Technol.*, **40**, 665 (2005).
- [38] D.J.Morrison, J.C.Moosbrugger; *Ins.J.Fatigue*, **19**, 551 (1997).
- [39] C.E.Feltner; *Tech.Document.Rep.No.RTD-TDR*, **63**, 4169 (1963).
- [40] C.Calabrese, C.Laird; *Mater.Sci.Eng.A*, **13**, 141 (1974).
- [41] M.Suery, B.B.Baudelet; *Phil.Mag.*, **41**, 41 (1980).
- [42] F.Abd El-salam, A.M.Abdelkhalekh, R.H.Nada, A.Fawzy; *Mater.Characterization*, **59**, 9 (2008).
- [43] A.F.Abd El-Rehim, M.A.Mahmoud; *J.Mater.Sci.*, **48**, 2059 (2013).